Visual Comput (2007) 23: 97–108
DOI 10.1007/s00371-006-0031-5

ORIGINAL ARTICLE

A vibrotactile approach to tactile rendering

Dennis Allerkamp
Guido Böttcher
Franz-Erich Wolter
Alan C. Brady
Jianguo Qu
Ian R. Summers

Published online: 11 July 2006

D. Allerkamp (✉) · G. Böttcher · F.-E. Wolter
Welfenlab, Division of Computer Graphics, University of Hannover
{allerkamp, boettcher, few}@gdv.uni-hannover.de

A.C. Brady · J. Qu · I.R. Summers
Biomedical Physics Group, School of Physics, University of Exeter
{alan.c.brady, j.qu, i.r.summers}@exeter.ac.uk

Abstract While moving our fingertip over a fine surface we experience a sensation that gives us an idea of its properties. A satisfactory simulation of this feeling is still an unsolved problem. In this paper, we describe a rendering strategy based on vibrations that play an important role in the tactile exploration of fine surfaces. To produce appropriate excitation patterns we use an array of vibrating contactor pins. Similar to the colour model in computer graphics, we simulate arbitrary vibrations as a superposition of only two sinewaves. Each sinewave is intended for the excitation of a specific population of mechanoreceptors. We carried out first tests of our rendering strategy on Brownian surfaces of different fractal dimensions.

Keywords Tactile rendering · Vibrotactile perception · Bistimulus theory · Brownian surfaces

1 Introduction

It is little known that the haptic sensory organ is the first one among the senses to be developed in a human embryo. However, it is well-known that in the virtual reality field systems supporting human tactile and haptic perception were the last ones to be investigated with some success and the whole field is far away from having reached some maturity. Our haptic and tactile sensory system has receptors in every part of the human skin and covers our body completely. As opposed to the visual and the hearing senses, the tactile sense cannot be shut down by blocking incoming signals as we can do it with the visual or acoustic senses by closing or covering the eyes and by using ear plugs. In any case, our haptic perception system is always active in all parts of our skin and this global sensory system communicates to us all the time comprehensively the mechanically felt sense of our very physical existence. All our senses work together in order to communicate to us relevant information that helps us to construct and update our internal model and our local habitat. Clearly, that internal model together with the permanent update enables us to be actively operational, including motion planning and performing very basic actions like grasping and touching and actively exploring any object we encounter.

Probably we are still at the very beginning of understanding and modelling appropriately all the relevant complex cognitive systems involved to accomplish the aforementioned basic orientation tasks. Here the problem to understand the basic cognitive systems may be split into several subtasks. One of them may concern the function and meaning of the local receptors of the outside world, the other subtask, which is perhaps even more difficult, may concern models explaining the global system functions that integrate the perception of the incoming signals to a global impression or global image. This paper focuses on tactile perception and employs and summarises

some partly recently established knowledge on functions of the tactile receptors in the human skin in Sect. 2. For the experiments described in this paper some insights concerning those receptors are especially important.

Tactile perception is usually considered crucial to complement the visual perception by confirming the feeling of what we see. Based on the understanding that this interaction between visual and tactile perception is extremely important, this paper reports on experiments where visual information contained in surface textures has been transformed into expected tactile signals conveying equivalent or at least compatible tactile perceptions occurring when touching those surface textures. Hence part of this paper deals with the generation of tactile signals creating the perceptions that are appropriate in the context of surface textures. To achieve the latter, some simplifying assumptions are made. The visual appearance of the texture of the surface (e.g., a textile) may have so-called symmetric well-ordered components created by repetitive structures. To classify the latter we consider here an important subclass of periodic 2-D geometric structures. Namely, we assume that the repetitive structure is created by a periodic parallel transformation of an elementary parallelogram that will be detected automatically. To this end, Sect. 5.1 describes strategies employing a combination of geometrical and stochastic methods to discover the elementary shape parallelogram. The latter basic geometric structure may then be used in repetition to create a simplified periodic structure. This may, e.g., happen by creating a dent texture using, e.g., a shape from a shading method to describe, e.g., a basic ovoid cap whose repetition creates the periodic structure.

A generally accepted taxonomy of textures (cf. [16]) assumes that apart from ordered components we can also recognise disordered unstructured components in surface textures. Considering the grey value image representing a surface texture, according to our model: In our human visual perception the unstructured parts of the latter grey value image are associated with different degrees of roughness that one would expect to feel if one were to touch the physical surface creating the particular surface texture. Those different degrees of expected roughness are classified by a parameter defined by a fractal dimension of the grey value image representing the surface texture. Employing the stochastic concept of Brownian motion it is possible to create height functions describing Brownian surfaces whose specific fractal dimensions can be prescribed by some stochastic parameters. The Brownian surface representing a surface with a specified roughness (fractal dimension) is finally used to create a tactile signal experienced by a person probing the Brownian surface with a stylus. More precisely, the person moves with a stylus over a virtual surface created by a phantom, i.e., a force feedback system that makes the user feel some resistance in case the probing stylus touches the virtual surface located in 3-D space. It is quite interesting that some preliminary experimental studies indicate that the perceived roughness intensity appears to increase strongly monotonously with the increase of the fractal dimension of the generated Brownian surface.

The tactile receptors in the human skin include the so-called pacinian and non-pacinian receptors. It is well-established that those two different receptors can be stimulated by vibrations. Moreover, it is well-known that the excitation intensity of that stimulation depends on the vibration frequency. According to our model in Sect. 5.4 there exist two different curves for the pacinian and non-pacinian receptors, respectively, describing for each vibration frequency the corresponding excitation intensity of the specific receptor type. The latter phenomenon has a counterpart in visual perception. In the tristimulus model (cf. [6]) the eye, or more specifically the retina, has three different receptors responding with different intensity to light with a given frequency. For each of the three visual receptors there exists a function obtained from measured data describing the stimulus intensity depending on the respective power associated with a specific frequency of the light. Practically valid models describing the type of colour perceived as stemming from the light reaching the human eye assume that the perceived colour is determined by the sum of the stimulation intensities experienced by all three receptors (cf. [4]). This implies the validity of the well-known RGB model. In the latter model, the total stimulation intensity is created by using light signals built up with three different colours corresponding to three basis frequencies only, where each of the three frequencies must be chosen with an appropriately adjusted energy. The model assumptions here lead to a three-dimensional model space describing all possibly perceivable colours. All those colours can be generated by "equivalent combinations" of any three different light sources, each of them radiating a different type of light with an appropriately chosen power depending on the power associated with the frequency distribution of the given three light sources. In this context it is only relevant that the three generated power/frequency distributions correspond to three linearly independent vectors (basis colours) representing equivalence classes of basis vectors in a 3-D vector space defined by vectors representing power/frequency distributions. This means that scaling each of the latter basis colour (light source) vectors with one appropriate positive real number will create any given total stimulation intensity perceived by the three receptors. This additive vector space concept useful for describing colour models is in Sect. 5.4 applied for modeling tactile sensations using two generating frequencies only. Analogue to the RGB model, we assume here that a "tactile colour" impression created by any vibration frequency distribution can be generated equivalently by the appropriately scaled intensities of two generating vibration frequencies (40 and 360 Hz) only. This is our current hypothesis in this paper, which still needs further experimental validation.

2 Human tactile perception

The skin being the biggest perceptional organ gives us the sense of touch. In contrast to our dominant senses like vision and hearing, touch requires an active exploration of the surrounding environment. By touching an object and moving over its surface, we receive information that is not obtainable by other senses. We can, for instance, assess the small-scale roughness of the surface, its softness and friction.

Located in the dermal and epidermal layer of the glabrous (hairless) skin, four different types of receptors send impulses to the somatosensory cortex, giving us the ability to estimate tactile quantities. Although each type of receptor reacts differently to mechanical stimuli applied on the skin (see Table 1), similarities have been observed in the rate of adaptation to a stimulus. The rate of adaptation represents the fall-off of neural activity during the presentation of a constant stimulus applied to the skin. A classification into two groups has been found: the fast adapting (FA) or rapid adapting receptors and the slow adapting receptors (SA). FA receptors are mostly sensitive to transients in skin deformation, whereas SA receptors also respond to sustained deformation.

Many experiments related to the sensitivity and firing rate of the receptors have been conducted in order to find the functional role of each receptor type in tactile perception. The results are summarised in [12]. Furthermore, the receptors differ by the size of their receptive field, i.e., the area of skin associated with a particular receptor within which a mechanical stimulus will excite that receptor. The correspondence between the receptive field and the spatial acuity has been studied extensively in order to investigate the mechanisms for texture discrimination.

Based on studies of the psychologist David Katz (see [14]), it is generally believed that two mechanisms are involved in the task of texture discrimination and roughness judgement. Depending on the size and distance of surface features one mechanism should dominate the other. The first mechanism is used on coarse textures where large skin displacements with relatively small changes over time occur. It is, therefore, believed that the Merkel discs as an SA receptor play an important role in discriminating these textures. The second mechanism should be relevant for fine textures where the skin experiences small displacements with many changes. Hence, it is assumed that vibrations inside the skin mediated by FA receptors are responsible for discrimination of fine textures. This two-mechanism hypothesis, the duplex theory, has been supported by experiments performed by Hollins et al. (see [10]). These suggest that vibratory perception in the pacinian channel is responsible for surface roughness judgements at structure sizes smaller than 100 μm, but this channel is not responsible for roughness perception at structure sizes greater than 100 μm.

By presuming a detection mechanism of vibrational components for microscopic structures, several experiments have been conducted from the acoustic point of view to investigate the mediation and detection of frequencies on the skin (see [3]). As a result, threshold curves have been found in [7] and [8] for each receptor, where every point describes an amplitude and frequency at which the stimulus was detected. Idealisation of those measurements result in the curves depicted in Fig. 13. We use the latter curves in Sect. 5.4 for the development of a model to describe "tactile colours" employing only two generating frequencies.

3 System overview

The goal of the HAPTEX project is the development of a virtual reality system for the visual and haptic presentation of textiles. The target scenario is depicted in Fig. 1. The virtual cloth is attached to a fixed stand. The user can touch, squeeze, rub and stretch the fabric with his thumb and index finger, feeling appropriate tactile stimulation at the fingertips.

The final goal is a very challenging task, because it must integrate force-feedback and tactile simulation posing more than only mechanical difficulties. Therefore, an intermediate scenario has been defined as a test bed for tactile rendering (see Fig. 2). Here the fabric is completely fixed on a rigid support. The user can tactually explore the fabric's surface with one fingertip. Force-feedback is not available, other than to define the plane of the surface.

Figure 3 gives an overview of the tactile rendering. Before any rendering can be done, the real fabric has to be converted into a virtual tactile fabric. Unlike real-time rendering, this preprocessing is not time critical. Thus it is desirable to do as much precomputation as possible to

Table 1. Characteristics of mechanoreceptors

Receptor type	Rate of adaptation	Receptive field	Function
Merkel discs	SA-I	small, well-defined	indentation, curvature
Ruffini's corpuscles	SA-II	large, undefined	static force, skin stretch
Meissner corpuscles	RA-I	small, well-defined	velocity, edges, slip detection
Pacinian corpuscles	RA-II	large, indistinct	acceleration, vibration

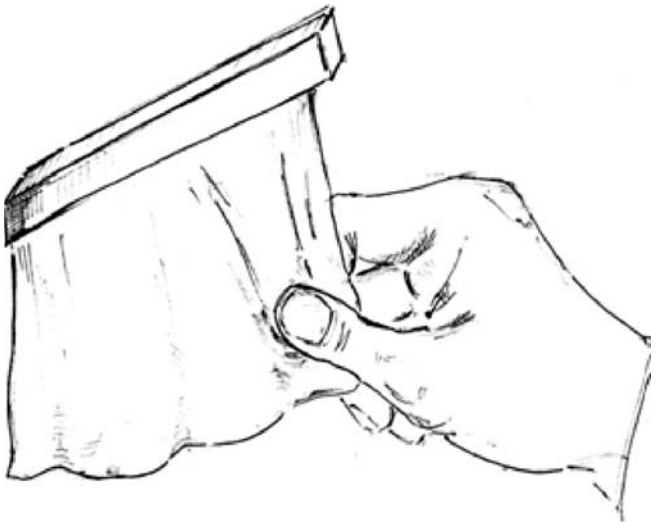

Fig. 1. HAPTEX final scenario

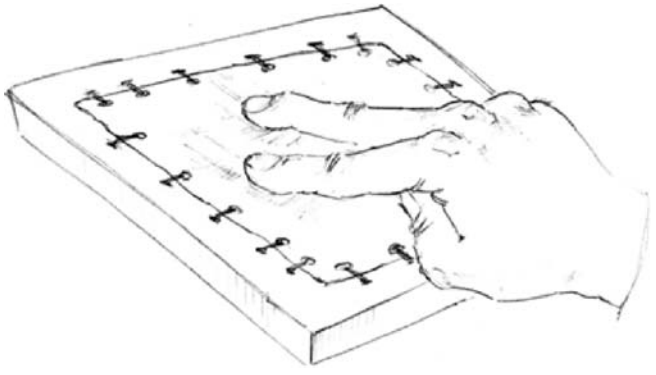

Fig. 2. HAPTEX tactile scenario

speed up the time critical rendering. A source of information about the fabric's surface is the appropriate Kawabata measurements as described in [15]. A way to convert these pure measurements into an appropriate virtual tactile fabric is described in [11]. Information regarding the fabric's surface can also be obtained from a high-resolution photography of the fabric. The latter task is described in more detail in Sect. 5.1.

Basically, the tactile renderer needs two ingredients to work properly: a computer representation of a fabric and the trajectory of the fingertip on the surface of the fabric. As described in Sect. 2, vibrotaction plays an important role in the perception of fine surface textures. Therefore, we compute the vibrations occurring in the fingertip while moving along the trajectory. These are decomposed into only two basic frequencies intended to directly stimulate the pacinian and non-pacinian receptors. We describe this process in Sect. 5. The stimulator hardware is described in Sect. 4.

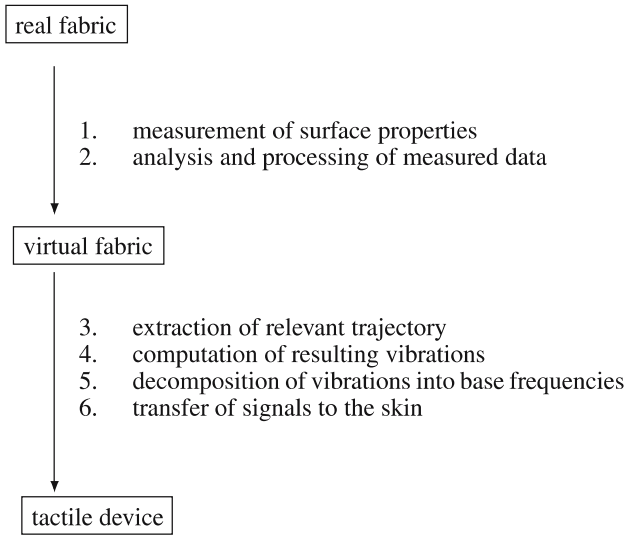

Fig. 3. Overview of the tactile rendering

4 Stimulator hardware

The stimulator under development for the HAPTEX project incorporates a pair of vibrotactile arrays, designed to produce touch sensations on the tips of the index finger and the thumb. These arrays are based on devices produced previously at the University of Exeter [18–20], with multiple contactors on the skin whose vibration waveform is under software control. The intention is to produce virtual touch sensations – edges and corners of objects, surface textures and contact area – by producing an appropriate spatiotemporal variation of mechanical disturbance over the skin. An array of this type does not aim to reproduce the topology of "real" surfaces, it aims to produce an appropriate excitation pattern over the various populations of mechanoreceptors in the skin.

Figure 4 shows an example of an earlier design – an array with 25 contactors over 1 cm^2 on the fingertip. This forms part of a 125-contactor, 5-digit stimulator for one hand. The contactor array, in the centre of the top surface, is driven by piezoelectric bimorphs (which appear black in the picture). Figure 5 shows an outline diagram of an array designed for the HAPTEX project. The finger is represented by the cylinder towards the top of the picture. Note that the mechanism is placed around the back of the finger so that there is minimum interference to manipulation.

The spatial resolution required for the contactor array is related to the density of mechanoreceptors in the skin, which is on the order of 1 mm^{-2} on the fingertip, or to the spatial acuity on the fingertip, which is around 1 mm [13]. In a previous investigation [19], using a 100-contactor array with a spatial resolution of 1 mm on the fingertip [18], we showed that it is difficult to discriminate between moving vibratory stimuli presented at resolutions

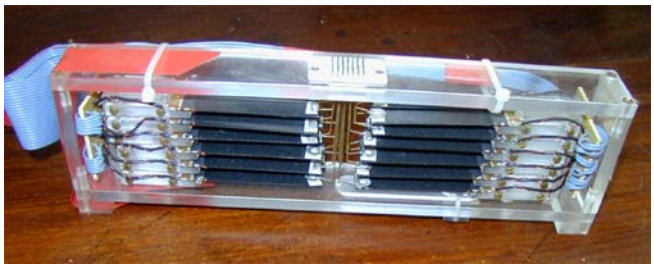

Fig. 4. Single-digit stimulator with 25 contactors over 1 cm^2 on the fingertip

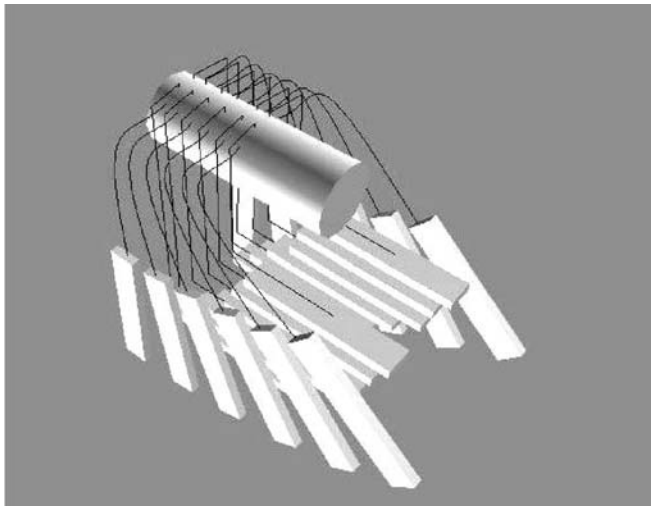

Fig. 5. Design for an array with 24 contactors over the fingertip

of 1 mm or 2 mm. This suggests that a 1 mm pitch array may offer little advantage over a 2 mm pitch array in some contexts. The proposed design for the arrays in the HAPTEX project has a contactor spacing of around 2 mm.

4.1 Electromechanical design

Electromechanical design may be facilitated by a mathematical model of the piezoelectric drive system and the mechanical load presented by the skin. For example, see Fig. 6, where the principle resonance of the system is represented by a simple mass-on-a-spring model. It is convenient to assume a linear model for the piezoelectric material and for the skin load – at large amplitudes both components are significantly non-linear, but for amplitudes less than 100 μm the linear assumption appears to produce valid predictions.

Figure 7 shows real, not model, data that were obtained via a miniature accelerometer from a single contactor in an array of the type shown in Fig. 4. The high-frequency limbs of such curves are dominated by the effective mass of the system (plus any load), and the low-

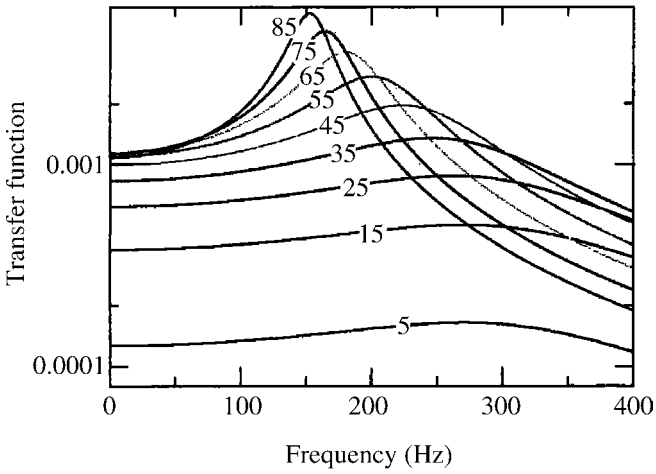

Fig. 6. Modelling of system frequency response, in the case of loading by the skin, for different lengths of piezoelectric drive element. (Labels indicate length in mm)

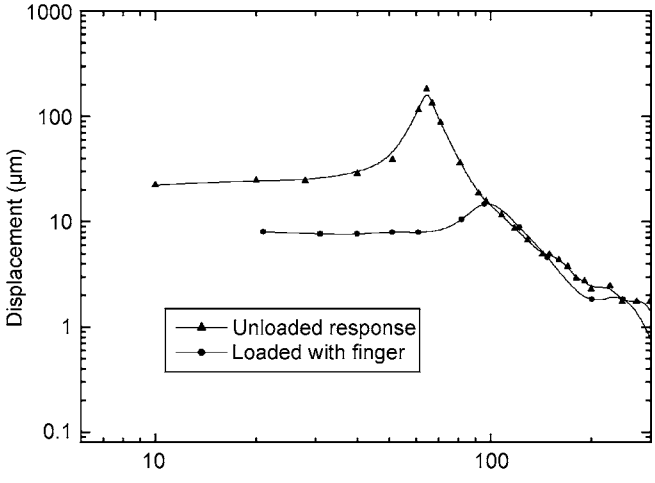

Fig. 7. The effect of skin load on the system frequency response

frequency limbs are dominated by the effective stiffness. The skin adds significant stiffness ($\sim 100\,\mathrm{Nm^{-1}}$) and resistance ($\sim 0.1\,\mathrm{Nm^{-1}s}$) to the system, but adds negligible effective mass ($\sim 10^{-5}$ kg), so the resonant frequency of the system is increased and the Q-factor is reduced. (The Q-factor relates to the width of the resonance: a high Q-factor means a narrow resonance.)

In order to evoke "realistic" touch sensations an array must operate over most of the tactile frequency range of, say, 10 to 500 Hz. Stimulation in the upper part of this frequency range is expected to stimulate mainly pacinian receptors. Stimulation at lower frequencies is expected to stimulate mainly non-pacinian receptors. To produce "comfortable" sensation levels requires a few microns at frequencies around 250 Hz and a few tens of microns at frequencies around 50 Hz.

4.2 Stimulus design

A significant problem for the operation of an array stimulator is the need to specify multiple parallel waveforms – there is essentially infinite choice within the system bandwidth. In an attempt to provide a user-friendly system, each waveform is constrained to be a specified mixture of 40 Hz and 320 Hz sinewaves, i.e., the output is a superposition of a spatiotemporal distribution of vibration at 40 Hz and a spatiotemporal distribution of vibration at 320 Hz.

The 40 Hz output is intended to stimulate primarily non-pacinian receptors and the 320 Hz output is intended to stimulate primarily pacinian receptors. This scheme was first proposed by Bernstein [2] in the context of single-channel vibrotactile stimulation. The two-frequency system may be considered as analogous to a 3-colour video display – the stimulator produces a sequence of frames in two tactile "colours". Psycho-physics experiments have been performed to compare the perception of moving stimuli at the two different stimulation frequencies [18]. Data were obtained on the masking of 40 Hz or 320 Hz stimuli by a uniform vibrating background at 40 Hz or 320 Hz. The two different stimulation frequencies produce different results, suggesting that different receptor populations have been targeted.

For stimuli at 40 Hz and 320 Hz to have the same subjective intensity, stimulus amplitude at 40 Hz must be around 10 times greater. For stimuli with components at both 40 Hz and 320 Hz, measurements have been made to determine the component amplitudes required to achieve constant subjective intensity as the amplitude ratio is varied. Figure 8 shows component amplitudes at 40 Hz and 320 Hz for constant subjective intensity. The data were averaged over five subjects, from a comparison between various two-component test stimuli and a two-component reference stimulus. The data have been fitted with an expression of the form $\left[(\frac{x}{a})^n + (\frac{y}{b})^n\right] = 1$, where $n = 1.23$ gives the best fit. Also shown are best-fit lines for a linear model ($n = 1$; the addition of normalised component amplitudes) and for an elliptical model ($n = 2$; the addition of normalised component powers). This experiment provides useful information for the control of subjective intensity in two-frequency stimuli. For stimulus components of 40 Hz and 320 Hz to have equal subjective intensity, the amplitude at 40 Hz must be approximately 20 times greater than the amplitude at 320 Hz (at least for the array and stimuli used in this experiment).

4.3 Drive electronics

For each of the contactors on the fingertip an appropriate driving signal has to be generated. We use a USB controller to produce the stimuli at the two different stimulation frequencies. This has two advantages: firstly, the intensities determined by the stimulator software can be simply transmitted to the controller via USB and secondly,

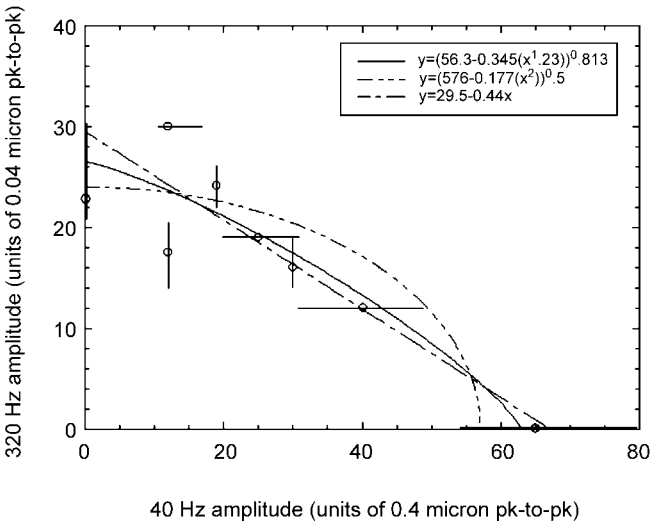

Fig. 8. Component amplitudes at 40 Hz and 320 Hz for constant subjective intensity

as the generation of the signals is implemented as a software program running on the USB controller, the format of the stimuli can be changed easily.

The created signals are transmitted to digital-to-analogue converters (DAC) via a bus system (see Fig. 9),

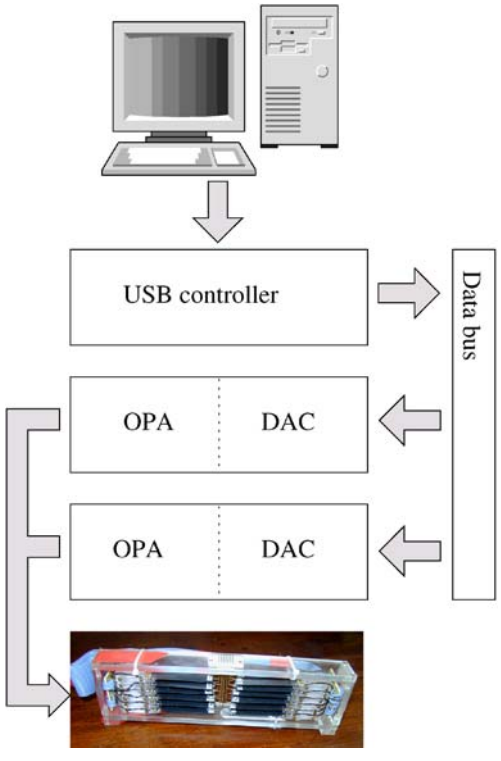

Fig. 9. Schematic of the drive electronics

which makes the system scaleable in the number of contactors being supported. We use high-voltage operational amplifiers (OPA) to amplify the output of the DACs to the levels (up to 40 V rms) required by the bimorphs.

5 Stimulator software

5.1 Analysis and processing of measured data

As a surface is two-dimensional by nature, we represent a fabric's surface as a two-dimensional property map $P(u, v)$. The descriptions of these properties depend on the mechanical model chosen for the virtual fabric. For simplicity, in the following discussion we represent the surface as rigid, with a specified height profile.

We describe a method that reconstructs a height function from a grey value image. The first step in this reconstruction process is the detection of symmetry in the grey value image. We define *symmetry* with regard to a set $\mathcal{P} \subseteq \mathcal{E}^2$ (with $\mathcal{E}^2$ denoting the Euclidean plane) as a bijective map $\alpha : \mathcal{E}^2 \to \mathcal{E}^2$ with $\alpha(\mathcal{P}) = \mathcal{P}$. Each symmetry of $\mathcal{E}^2$ is a translation, rotation, reflection or glide reflection. The symmetries of most fabrics are a combination of two non-parallel translations. These translations define a basic element called tile that is repeated in the translational directions (see Fig. 10). An algorithm for finding such a tile was implemented based on [9] at the Welfenlab. As the symmetries are not perfect in general, stochastic methods are used to find an idealised tiling.

Since the tile is repeated on the grey value image, we use the average of these repetitions to create a new synthetic image of the surface, thus being cleaned from noise. This image in turn is used as input for a shape-from-shading algorithm (see [21]) that computes an appropriate height profile. See Fig. 11 for an example.

5.2 Extraction of relevant trajectory

In our model (see Fig. 12) every contactor of the tactile array is assigned a two-dimensional device coordinate $\begin{pmatrix} x_i \\ y_i \end{pmatrix}$. Let $\begin{pmatrix} 0_u(t) \\ 0_v(t) \end{pmatrix}$ denote the position of the origin of the device coordinate system on the fabrics surface (trajectory) and $\varphi(t)$ the angle between the x-axis and the u-axis at the time t, then the position of the contactors on the fabric's surface can be computed with

$$\begin{pmatrix} u_i(t) \\ v_i(t) \end{pmatrix} = \begin{pmatrix} 0_u(t) \\ 0_v(t) \end{pmatrix} + \begin{pmatrix} \cos\varphi(t) & -\sin\varphi(t) \\ \sin\varphi(t) & \cos\varphi(t) \end{pmatrix} \begin{pmatrix} x_i \\ y_i \end{pmatrix}$$

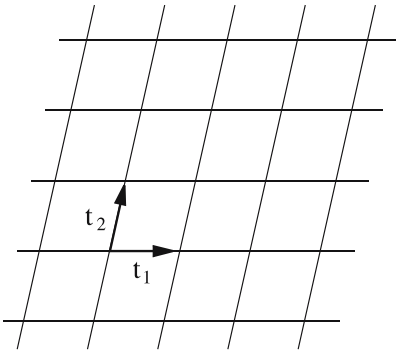

Fig. 10. Tile with translations t_1 and t_2

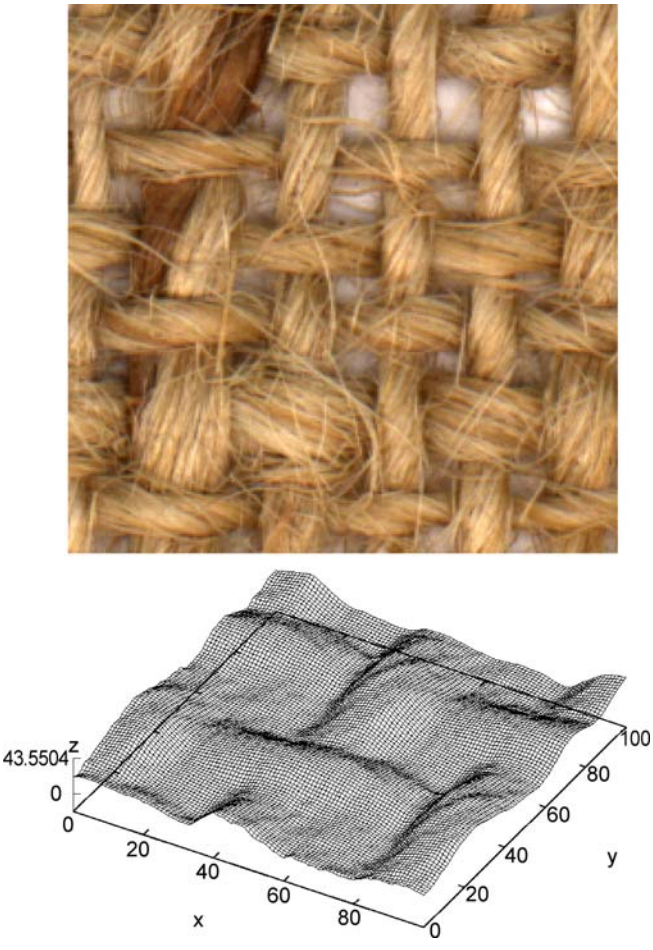

Fig. 11. Photograph of a fabric and the corresponding height profile

Using the property map $P(u, v)$ we can now define the time dependent property function $P_i(t) := P(u_i(t), v_i(t))$ along the trajectory.

As we are rendering the device signals for the next 25-ms time frame we presumably need to extrapolate the trajectory beyond the current time.

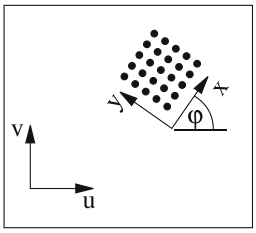

Fig. 12. Tactile contactors on the fabric surface

5.3 Computation of resulting vibrations

For each contactor we need to compute the vibrations occurring due to the movement of the fingertip over the surface. This computation depends on the model used in Sect. 5.1. Since we represent the surface as a height function, $P_i(t)$ describes the height under the i-th contactor as a function of time. As a start we act on the simple assumption that the vibration at the contactor position on the finger directly corresponds to $P_i(t)$. We want to express a vibration as a function F by assigning to each frequency ω a corresponding amplitude $F(\omega)$, which is done by Fourier transforming $P_i(t)$. Since we need to render the device signals for the next 25 ms, this time segment becomes our window for the Fourier transform. We smooth the boundaries of this segment with a Blackman window.

5.4 Decomposition of vibrations into base frequencies

The previous steps result in a frequency spectrum $F(\omega)$, which now has to be decomposed into amplitudes at only two base frequencies that will then be reproduced on the tactile stimulator. We use 40 Hz and 320 Hz as base frequencies (see Sect. 4). The function mapping the spectrum to these two amplitudes has to ensure that the resulting tactile sensation is very similar to the sensation that would result from reproducing the whole spectrum on the tactile stimulator. This approach is analogous to the approach used for multicolour video displays, which produce almost arbitrary colours as mixtures of only three fundamental colours.

Similar to the colour model of computer graphics (e.g., see [6]), we assume the existence of two functions H_{40} and H_{320} such that the two amplitudes for 40 and 320 Hz can be computed as an integral of a convolution:

$$a_{40} = \int H_{40}(\omega) \cdot F(\omega) \mathrm{d}\omega\,,$$
$$a_{320} = \int H_{320}(\omega) \cdot F(\omega) \mathrm{d}\omega\,. \tag{1}$$

This hypothesis still has to be verified with appropriate experiments. Nevertheless, in the rest of this section we will show the reasonableness of this approach and we will even derive first approximations of the functions H_{40} and H_{320}.

With $\mathit{l}_p(F)$ and $\mathit{l}_{np}(F)$ we denote the stimulation intensity caused by a vibration with spectrum function F at the pacinian and non-pacinian channel, respectively. Note that these intensity functions are subjective and thus hard to define. Our suggestion for an approximation of these functions is

$$\mathit{l}_p(F) = \int \frac{F(\omega)}{T_p(\omega)} \mathrm{d}\omega$$
$$\mathit{l}_{np}(F) = \int \frac{F(\omega)}{T_{np}(\omega)} \mathrm{d}\omega\,. \tag{2}$$

Since the channels react depending on the frequency (e.g., the pacinian channel is most sensitive around 300 Hz, while the non-pacinian channel is most sensitive around 50 Hz), we use $\frac{1}{T_p(\omega)}$ and $\frac{1}{T_{np}(\omega)}$ as frequency dependent damping factors. The assignment of a linear factor to each frequency seems to be a reasonable approximation suggested by some curves of equal sensation magnitude plotted as a function of stimulus frequency (see [22]). Furthermore, the approach of using an integral is supported by assuming $n = 1$, i.e., a linear model in Sect. 4.2.

In [7] thresholds of the tactile channels as functions of stimulus frequency were measured (see Fig. 13 for approximating curves). These thresholds refer to the smallest perceivable amplitude of a stimulus with only a single frequency. Along these measured curves, the intensity is considered to be constant, making these functions suitable as frequency dependent damping functions $T_p(\omega)$ and $T_{np}(\omega)$ that normalise the intensity to 1 at threshold level.

Let

$$S_{\bar{\omega},\alpha}(\omega) = \begin{cases} \alpha & \text{for } \omega = \bar{\omega} \\ 0 & \text{else} \end{cases}$$

denote a simple sinusoidal vibration with frequency $\bar{\omega}$ and amplitude α. Our goal is to replace a given vibration F by

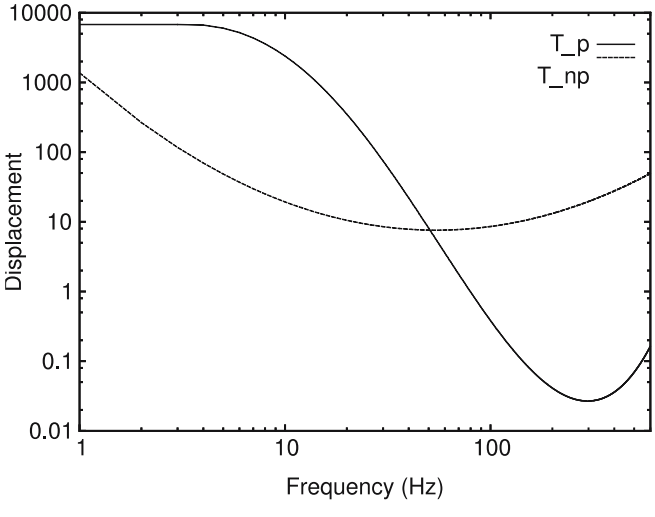

Fig. 13. The functions T_p and T_{np}

two vibrations $S_{40,a_{40}}$ and $S_{320,a_{320}}$ such that

$$\mathcal{I}_p(F) = \mathcal{I}_p(S_{40,a_{40}}) + \mathcal{I}_p(S_{320,a_{320}}) ,$$
$$\mathcal{I}_{np}(F) = \mathcal{I}_{np}(S_{40,a_{40}}) + \mathcal{I}_{np}(S_{320,a_{320}}) .$$

These equations are equal to a two-dimensional linear equation system (with Eq. 2):

$$\int \frac{F(\omega)}{T_p(\omega)} \mathrm{d}\omega = \frac{a_{40}}{T_p(40)} + \frac{a_{320}}{T_p(320)}$$
$$\int \frac{F(\omega)}{T_{np}(\omega)} \mathrm{d}\omega = \frac{a_{40}}{T_{np}(40)} + \frac{a_{320}}{T_{np}(320)} .$$

The solutions of this system have the form

$$a_{40} = B_{11} \cdot \int \frac{F(\omega)}{T_p(\omega)} \mathrm{d}\omega + B_{12} \cdot \int \frac{F(\omega)}{T_{np}(\omega)} \mathrm{d}\omega$$
$$a_{320} = B_{21} \cdot \int \frac{F(\omega)}{T_p(\omega)} \mathrm{d}\omega + B_{22} \cdot \int \frac{F(\omega)}{T_{np}(\omega)} \mathrm{d}\omega .$$

Setting

$$H_{40}(\omega) := \frac{B_{11}}{T_p(\omega)} + \frac{B_{12}}{T_{np}(\omega)} ,$$
$$H_{320}(\omega) := \frac{B_{21}}{T_p(\omega)} + \frac{B_{22}}{T_{np}(\omega)} ,$$

we obtain Eq. 1. H_{40} and H_{320} are depicted in Fig. 14.

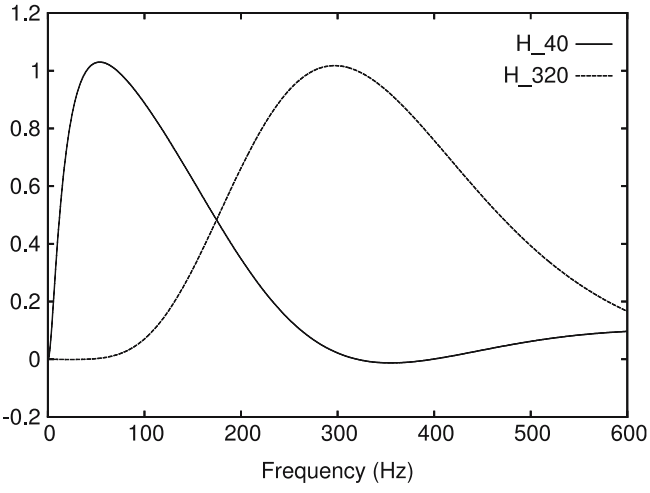

Fig. 14. The functions H_{40} and H_{320}

6 Brownian surfaces

In order to test our rendering strategy, we carried out a preliminary experiment using a tactile array to present synthetically generated Brownian surfaces with varying fractal dimensions. It is shown in [1] that there exists a strong correlation between the fractal dimension of a haptic texture and the impression of roughness perceived by tactually exploring it with a pen-like probe. We will get back to this later in this section. First we will present one of the various ways of defining a fractal dimension, the Hausdorff dimension.

6.1 Fractal dimension

Let $F \subseteq \mathbb{R}^n$, $F \neq \emptyset$ with $d(x, y)$ denoting the Euclidean distance in $\mathbb{R}^n$. Then $\mathrm{diam}(F) := \sup\{d(x, y) | x, y \in F\}$ is called the *diameter* of F.

Let $\delta \in \mathbb{R}^+$ and $\{U_i\}_{i\in\mathbb{N}}$ be a countable set of subsets of $\mathbb{R}^n$ with $\mathrm{diam}(U_i) \leq \delta$. Then $\{U_i\}_{i\in\mathbb{N}}$ is called a δ-*cover* of F if $F \subset \bigcup_{i=1}^{\infty} U_i$.

Let $s \in \mathbb{R}^+$. For every $\delta \in \mathbb{R}^+$:

$$\mathcal{H}^s_\delta(F) := \inf \left\{ \sum_{i=1}^{\infty} (\mathrm{diam}(U_i))^s | \{U_i\}_{i\in\mathbb{N}} \ \delta\text{-cover of } F \right\} .$$

Then the *s-dimensional Hausdorff measure* is defined as

$$\mathcal{H}^s := \lim_{\delta \to 0} \mathcal{H}^s_\delta(F) .$$

Hausdorff proved the existence of a number D_F fulfilling

$$\mathcal{H}^s(F) = \begin{cases} \infty & \text{for } s < D_F \\ 0 & \text{for } s > D_F . \end{cases}$$

Now we can define the *Hausdorff dimension* $\dim_H(F)$ as

$$\dim_H(F) := \inf\{s | \mathcal{H}^s(F) = 0\} = \sup\{s | \mathcal{H}^s(F) = \infty\} .$$

The Hausdorff dimension $\dim_H(F)$ has some basic properties:

- If $F \subset \mathbb{R}^n$, then $\dim_H(F) \leq n$.
- If $F \subset G$, then $\dim_H(F) \leq \dim_H(G)$.
- If F is countable, then $\dim_H(F) = 0$.

6.2 Generation of Brownian surfaces

We show how textures with given fractal dimension are generated.

A *Brownian surface* $X_H(x, y)$ ($X_H : \mathbb{R}^2 \to \mathbb{R}$) with *index* H ($0 \leq H \leq 1$) is a stochastic process where:

1. $X_H(0, 0) = 0$.
2. $X_H(x, y)$ is continuous.
3. Let $\sigma, \tau \geq 0$. Then the increments $X_H(x+\sigma, y+\tau) - X_H(x, y)$ are normally distributed with expectation 0

and variance $(\sigma^2+\tau^2)^H =: \rho$, i.e.,

$$P(X_H(x+\sigma, y+\tau) - X_H(x, y) \le z) = (2\pi)^{-\frac{1}{2}}(\rho)^{-\frac{1}{2}} \int_{-\infty}^{z} \exp\left(-\frac{r^2}{2\rho}\right) \mathrm{d}r\,.$$

$X_H(x, y)$ itself is also normally distributed with expectation 0 and variance $(x^2+y^2)^H$. Figure 15 shows some examples of Brownian surfaces with different indices. It is shown in [5] that a Brownian surface $X_H(x, y)$ with index H has Hausdorff and box dimensions $\dim_H X_H(x, y) = \dim_B X_H(x, y) = 3 - H$. In the following, we refer to these dimensions in brief as fractal dimension $\dim X_H(x, y)$.

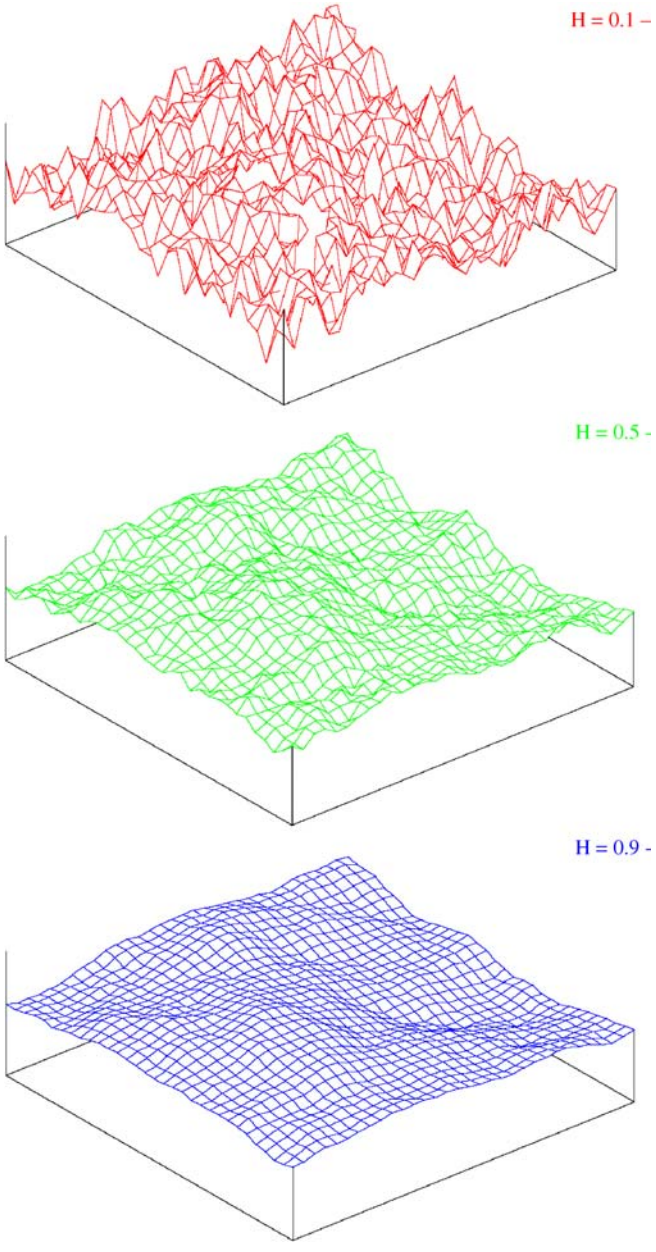

Fig. 15. Brownian surfaces with index 0.1 (red), 0.5 (green) and 0.9 (blue)

A Brownian surface with $(x, y) \in [0, 1] \times [0, 1]$ can be constructed with the following algorithm (see [17]):

1. Set $X_H(0, 0) = 0$ and randomly draw $X_H(0, 1)$, $X_H(1, 0)$ and $X_H(1, 1)$ from a normal distribution with expectation 0 and variance 1.
2. Iterate over (i, j) and randomly draw $X_H(k2^{-i}, l2^{-j})$ from a normal distribution with expectation

$$\frac{1}{4}\big[X_H((k-1)2^{-i}, (l-1)2^{-j}) + X_H((k-1)2^{-i}, (l+1)2^{-j}) + X_H((k+1)2^{-i}, (l-1)2^{-j}) + X_H((k+1)2^{-i}, (l+1)2^{-j})\big]$$

and variance

$$2^{(-i-j)H}\,.$$

The variables k, l, i and j have to satisfy

$$0 \le k \le 2^i, \quad i \ge 1, \quad k \text{ odd and}$$
$$0 \le l \le 2^j, \quad j \ge 1, \quad l \text{ odd}\,.$$

Because of the continuity of $X_H(x, y)$, the resulting surface is completely determined.

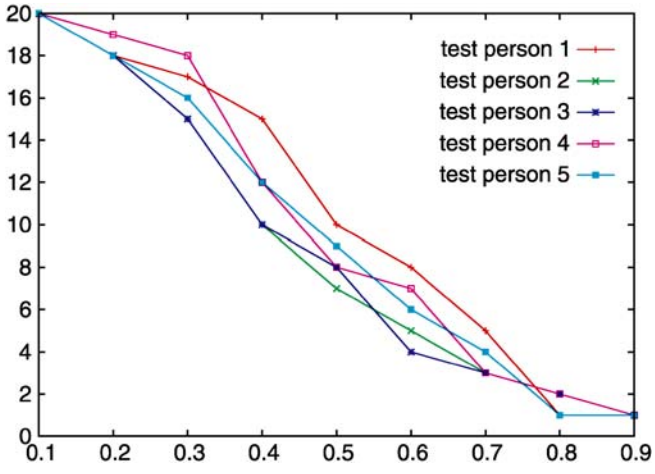

Fig. 16. Results of the experiment with the indices H of the Brownian surfaces on the abscissa and the impression of roughness on the ordinate (with 20 corresponding to the roughest and 1 to the smoothest surface)

6.3 Fractal dimension determines impression of roughness

The correlation between the fractal dimension and the impression of roughness was investigated in an experiment at the Welfenlab, using a single-point contact with the virtual surface. The PHANToM® device was used to simulate the feel of surfaces with different indices H. The test subjects could use a pen-like probe to explore the surfaces. To permit comparability, the smoothest and the roughest surfaces were presented and they were given fixed roughness values of 1 and 20. The test persons were asked to rate randomly chosen surfaces inside this range.

Figure 16 shows some results of this experiment. As one can see, there exists a strong correlation between the fractal dimension of a haptic texture $X_H(X, Y)$, i.e., $\dim X_H(x, y) = 3 - H$ and the impression of roughness received by tactually exploring it.

6.4 First results using a tactile array

We used the generated Brownian surfaces to test our vibrotactile rendering strategy described in Sects. 5.2, 5.3 and 5.4. Since the system was not yet fully operable for active exploration of a surface in real time, we used a passive presentation – stimuli were presented to the stationary fingertip, computed for the case of the virtual surface moving over the fingertip at a constant speed of 8 cm s^{-1}. As expected from the single-point-contact experiment, different Brownian surfaces were distinguished on the basis of roughness corresponding to the fractal dimension. However, there was little or no sensation of movement over the fingertip (presumably because individual surface features were not sufficiently identifiable to allow them to be tracked as they moved over the array). In the case of the active exploration envisaged for the fully operable system, the sensation of movement would be available from kinaesthetic and visual clues, and so the results would presumably be more convincing.

7 Conclusion

With careful attention to design it is possible to produce effective array stimulators. These may be used in conjunction with force-feedback devices to provide multipoint (distributed) tactile stimulation as an enhancement to single-point display of gross mechanical properties. The principal problem in implementation derives from a lack of information about the relation between the surface topology of an object being touched and the consequent time-varying distribution of mechanical excitation over the various populations of mechanoreceptors in the skin. A possible model of this relation is presented in this paper, allowing drive waveforms for an array to be derived from real-time information about the user's movements and prior knowledge of the (virtual) surface being explored. The model is awaiting full experimental validation within the HAPTEX project, in terms of its ability to produce realistic virtual sensations, but the overall system incorporates sufficient flexibility for the model to be developed as required.

Acknowledgement The project "HAPtic sensing of virtual TEXtile" (HAPTEX) is a research project funded under the Sixth Framework Programme (FP6) of the European Union (Contract No. IST-6549). The funding is provided by the Future and Emerging Technologies (FET) Programme, which is part of the Information Society Technologies (IST) programme and focuses on novel and emerging scientific ideas. Its mission is to promote research that is of a long-term nature or involves particularly high risks, compensated by the potential of a significant societal or industrial impact.

Figures 1 and 2 were kindly provided by PERCRO, Scuola Superiore S.Anna, Pisa. The data in Fig. 8 were obtained in Exeter by Dr M.K. Syed.

References

1. Bergmann, M., Herbst, I., von Wieding, R., Wolter, F.E.: Haptical rendering of rough surfaces using their fractal dimension. In: Proceedings of the First PHANToM Users Research Symposium, pp. 9–12. German Cancer Research Center, Heidelberg, Germany (1999)
2. Bernstein, L.E., Eberhardt, S.P., Demorest, M.E.: Single-channel vibrotactile supplements to visual perception of intonation and stress. J. Acoust. Soc. Am. **85**, 397–405 (1989)
3. Bolanowski, S.J., Gescheider, G.A., Verillo, R.T., Checkowsky, C.M.: Four channels mediate the mechanical aspects of touch. J. Acoust. Soc. Am. **84**, 1680–1694 (1988)
4. Cornsweet, T.N.: Visual Perception. Academic Press, New York (1970)
5. Falconer, K.J.: Fractal geometry: mathematical foundations and applications. Wiley, Chichester (1990)
6. Foley, J.D., van Dam, A., Feiner, S.K., Hughes, J.H.: Computer Graphics: Principles and Practice, 2nd edn. Addison-Wesley, Reading, MA (1996)
7. Gescheider, G.A., Bolanowski, S.J., Pope, J.V., Verillo, R.T.: A four-channel analysis of the tactile sensitivity on the fingertip: frequency selectivity, spatial summation, and temporal summation. Somatosens. Mot. Res. **19**(2), 114–124 (2002)
8. Gescheider, G.A., Bolanowski, S.J., Verrillo, R.T.: Some characteristics of tactile channels. Behav. Brain Res. **148**, 35–40 (2004)
9. Handley, C.: The analysis and reconstruction of repetitive textures. In: Proceedings: Computer Graphics International, pp. 273–276, IEEE (1998)
10. Hollins, M., Bensmaïa, S.J., Washburn, S.: Vibrotactile adaption impairs discrimination of fine, but not coarse, textures. Somatosens. Mot. Res. **18**(4), 253–262 (2001)
11. Huang, G., Metaxas, D., Govindaraj, M.: Feel the "fabric": an audio-haptic interface. In: SCA '03: Proceedings of the 2003 ACM SIGGRAPH/Eurographics Symposium on Computer animation, pp. 52–61. Eurographics Association (2003)
12. Johnson, K.O.: The roles and functions of cutaneous mechanoreceptors. Curr. Opin. Neurobiol. **11**, 455–461 (2001)

13. Johnson, K.O., Yoshioka, T., Vega-Bermudez, F.: Tactile functions of mechanoreceptive afferents innervating the hand. J. Clin. Neurophysiol. **17**(6), 539–558 (2000)
14. Katz, D.: The World of Touch. Lawrence Erlbaum Associates, Mahwah, MJ (1989)
15. Kawabata, S.: The standardization and analysis of hand evaluation. Technical Report, The Hand Evaluation and Standardization Committee, The Textile Machinery Society of Japan (1980)
16. Rao, A.R.: A Taxonomy for Texture Description and Identification, 1st edn. Springer, Berlin Heidelberg New York (1990)
17. Schulze, M.: Von computergraphischen zu haptischen Texturen. Virtual Reality für den Entwicklungsbereich Design/Styling in der Automobilindustrie. Ph.D. Thesis, Universität Hannover (2005)
18. Summers, I.R., Chanter, C.M.: A broadband tactile array on the fingertip. J. Acoust. Soc. Am. **112**(5), 2118–2126 (2002)
19. Summers, I.R., Chanter, C.M., Southall, A.L., Brady, A.C.: Results from a tactile array on the fingertip. In: Proceedings of Eurohaptics 2001, pp. 26–28 (2001)
20. Summers, I.R., Whybrow, J.J., Milnes, P., Brown, B.H., Stevens, J.C.: Tactile perception: comparison of two stimulation sites. J. Acoust. Soc. Am. **118**(4), 2527–2534 (2005)
21. Tsai, P.S., Shah, M.: Shape from shading using linear approximation. Image Vis. Comput. **12**(8), 487–498 (1994)
22. Verrillo, R.T., Fraioli, A.J., Smith, R.L.: Sensation magnitude of vibrotactile stimuli. Percept. Psychophys. **33**, 379–387 (1969)






DENNIS ALLERKAMP studied Mathematics and Computer Science at the University of Hanover and wrote his diploma thesis on the Computation of Medial Sets of Curved Surfaces in Euclidean Space. He received his Diploma in Mathematics (Master's equivalent) in December 2004. Since then he has been working at the Computer Graphics Department of the University of Hannover as a research assistant and Ph.D. candidate. His research interests are in the areas of haptics, human-computer interfaces, as well as medial axis. Currently, he is mainly involved in the HAPTEX project.

GUIDO BÖTTCHER studied Mathematics and Computer Science at the University of Hanover and wrote his diploma thesis on medial axis and haptics. He received his Diploma in Mathematics (Master's equivalent) in January 2005. Since then he has been working at the Division of Computer Graphics of the University of Hannover as a research assistant and PhD candidate. Currently, he is mainly involved in the HAPTEX project.

ALAN C. BRADY studied Chemistry and Physics at Exeter, and in 1996 received his MPhil for work on Molecular Rectification in Langmuir–Blodgett films. In 2000 he joined the Biomedical Physics Group to work on new tactile interfaces and to study the psychophysics of touch. He is currently involved in the HAPTEX, ENACTIVE and ROSANA projects.

JIANGUO QU obtained his BSc and MSc in textile/control at Tianjin Polytechnic University in 1982 and 1987, respectively, and his PhD in clothing at Manchester Metropolitan University in 2003. He previously worked at HebeiKeji University as a lecturer in 1982–1995 and an associate professor in 1995–1999. He also worked as a research associate at Manchester Metropolitan University in 2002–2003 and at Loughborough University in 2004. He is currently working as a postdoctoral research fellow on the HAPTEX project at the School of Physics at Exeter University.

IAN R. SUMMERS is a member of the Biomedical Physics Group at the University of Exeter, UK. He is also Director of the Peninsula MR Research Centre in Exeter, and is involved with undergraduates and postgraduate programmes in Physics and Radiography. His research interests include functional magnetic-resonance imaging, auditory perception and tactile perception. He has worked in the area of touch perception for over 25 years. His research group in Exeter has developed a wide range of novel tactile stimulators, including stimulator arrays for producing virtual touch sensations on the fingertip.

FRANZ-ERICH WOLTER has been a full professor of Computer Science at the University of Hannover since the winter term of 1994/1995, where he is the director of the Division of Computer Graphics and Geometric Modeling, called Welfenlab. Before coming to Hannover, Dr. Wolter held faculty positions at the University of Hamburg (in 1994), MIT (1989–1993) and Purdue University in the USA (1987–1989). Prior to this, he developed industrial expertise as a software and development engineer with AEG in Germany (1986–1987). Dr. Wolter obtained his PhD in 1985 from the Department of Mathematics at the Technical University of Berlin, Germany, in the area of Riemannian manifolds. In 1980 he graduated in Mathematics and Theoretical Physics from the Free University of Berlin. At MIT Dr. Wolter co-developed the geometric modeling system Praxiteles for the US Navy from 1989 to 1993 and published various papers that broke new ground applying concepts from differential geometry and topology on problems and design of new methods used in geometric modeling and CAD systems. Dr Wolter is a research affiliate of the MIT Department of Mechanical Engineering.